

# Symmetry-protected Bose-Einstein condensation of interacting hardcore bosons

R. H. Wilke,<sup>1</sup> T. Köhler,<sup>2</sup> F. A. Palm,<sup>1</sup> and S. Paeckel<sup>1</sup>

<sup>1</sup>*Department of Physics, Arnold Sommerfeld Center for Theoretical Physics (ASC),  
Ludwig-Maximilians-Universität München, 80333 München, Germany*

<sup>2</sup>*Department of Physics and Astronomy, Uppsala University, Box 516, S-751 20 Uppsala, Sweden  
(Dated: March 29, 2022)*

We introduce a mechanism stabilizing a one-dimensional quantum many-body phase, characterized by a certain wave vector  $k_0$ , from a  $k_0$ -modulated coupling to a center site, via the protection of an emergent  $\mathbb{Z}_2$  symmetry. We illustrate this mechanism by constructing the solution of the full quantum many-body problem of hardcore bosons on a wheel geometry, which are known to form a Bose-Einstein condensate. The robustness of the condensate is shown numerically by adding nearest-neighbor interactions to the wheel Hamiltonian. We identify the energy scale that controls the protection of the emergent  $\mathbb{Z}_2$  symmetry. We discuss further applications such as geometrically inducing finite-momentum condensates. Since our solution strategy is based on a generic mapping from a wheel geometry to a projected ladder, our analysis can be applied to various related problems with extensively scaling coordination numbers.

Cold atom experiments have become a versatile platform to realize various exotic quantum phases of matter [1–8]. Available experimental setups nowadays allow for the control of both geometry and interactions of simulated model systems. It is thus crucial to theoretically identify physical mechanisms that improve the stability and scaling properties of exotic quantum phases, which then might be realized and tested in experiments. In that context, remarkable progress in understanding the stability of Bose-Einstein condensate (BEC) has been made by analyzing spectral properties of a wheel of hardcore bosons (HCB) [9–12] as depicted in Fig. 1a. This model features an energy scale  $\sim \sqrt{L}$  that is generated by the extensively scaling coordination number of a center site. While large coordination numbers appear in several theoretical approaches [13–18], the exact solution as well as the stability against perturbations remained an open question. Besides others, the problem of finding exact expressions for ground states of long-range coupled HCB Hamiltonians is a major obstacle. Here, arbitrarily long-ranged interactions appear when expressing the HCB degrees of freedom in terms of spinless fermions (SF) via a Jordan-Wigner transformation (JWT).

In this letter, we present a mapping that allows us to construct the full solution of a family of quantum many-body problems with arbitrary  $k_0$ -modulated ring-to-center hoppings  $s_j = se^{ik_0j}$ , and to analyze the formation of a BEC phase with momentum  $k_0$ . In the context of central spin models [19–24] a solution strategy to a similar problem is based on the Bethe ansatz and has been applied to describe for instance Rydberg impurities in ultracold atomic quantum gases [25]. In contrast, we derive the solution by introducing a mapping to a ladder system of SF, yielding closed analytical expressions. We emphasize that this mapping can be applied in various other setups to analytically tackle problems with an extensively scaling coordination number. In the context of hardcore bosons, our approach reveals that the sta-

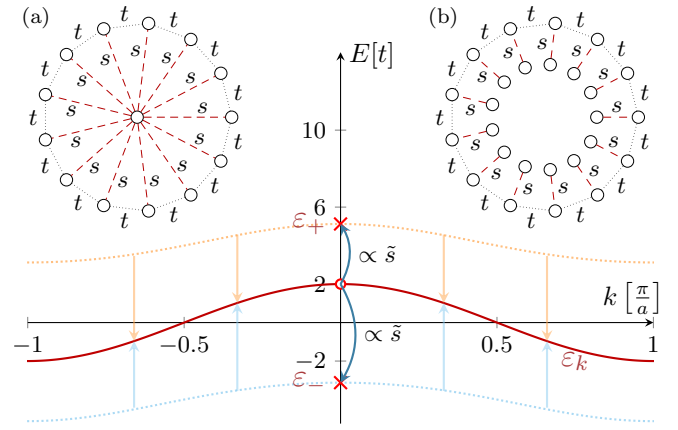


FIG. 1. The main plot illustrates the single-particle dispersion relation (middle, red curve) of the wheel geometry (a), emerging from projecting down the dispersion from the ladder geometry (b) (upper orange and lower blue curve). Note the appearance of two single-particle states at  $k_0 = 0$  (red crosses). This is because the Hilbert space of the wheel is obtained by projecting out all modes on the inner ring, except for the zero momentum states  $|N_{\odot, k=0}\rangle_{\odot}$ . Momentum conservation then couples this central mode to the particular mode on the outer ring respecting the  $k_0$ -modulated ring-to-center hopping, which generates an extensively scaling level splitting (red circle and crosses).

bilizing mechanism for the BEC is the extensively scaling coordination number of the center site, introducing a robust discrete  $\mathbb{Z}_2$  symmetry that protects the ordered quantum many-body phase against local perturbations on the outer ring. Furthermore, we trace back the protection to odd-parity  $k = k_0$  single-particle states that are gapped out  $\sim s\sqrt{L} \equiv \tilde{s}$ . This property allows us to show that in the thermodynamic limit the system immediately transitions into a BEC, as long as there is a finite ring-to-center hopping rate  $s > 0$ , which remarkably also holds when adding local interactions to the outer ring. We

demonstrate, beyond previous work, the robust protection of the BEC numerically, using density-matrix renormalization group (DMRG) [26, 27] simulations to calculate the  $k_0$ -condensate fraction when adding nearest-neighbor (NN) interactions, for a wide parameter range and various particle densities. As a consequence, the  $\mathbb{Z}_2$  symmetry in principle allows to experimentally tune the transition temperature of a gas of interacting HCB by modifying the wheel's coordination number. Here, we show that the central quantity is the ratio  $\frac{V}{\tilde{s}}$  between the interaction strength  $V$  and the renormalized ring-to-center hopping, which we demonstrate by further numerical results. Finally, our analysis implies that the emergent  $\mathbb{Z}_2$  symmetry is generically induced by the model's geometry. Therefore, general  $k_0$ -modulated hoppings give rise to corresponding protected  $k_0$ -modes and the respective single-particle states are gapped out  $\sim s\sqrt{L}$ . This paves the way to a generic mechanism that can be exploited in various contexts, for instance, to stabilize exotic quantum many-body phases such as  $k_0 \neq 0$  BEC [28–31].

*Analytical solution via wheel-to-ladder mapping.*— We consider HCB on a  $L$ -sited ring with an additional center site [10, 12] (see Fig. 1a). The model exhibits  $k_0$ -modulated ring-to-center hopping  $s_j = se^{ik_0j}$  while the homogeneous hopping on the ring is tuned by a parameter  $t$ . The corresponding Hamiltonian reads

$$\hat{H} \equiv -t \sum_{j=0}^{L-1} \left( \hat{h}_j^\dagger \hat{h}_{j+1} + \text{h.c.} \right) - \sum_{j=0}^{L-1} \left( s_j \hat{h}_j^\dagger \hat{h}_\odot + \text{h.c.} \right), \quad (1)$$

where  $\hat{h}_j^{(\dagger)}$  is the HCB ladder operator on the  $j$ -th site of the ring and  $\hat{h}_\odot^{(\dagger)}$  on the center site, spanning the overall Hilbert space  $\mathcal{H}_2^{\otimes L+1}$ . In the limit  $\frac{s}{t} \rightarrow 0$  (ring geometry) the model exhibits a quasi BEC, i.e., the ground state is a bosonic condensate, whose occupation scales as  $\sqrt{N}$  [32, 33], where  $N$  denotes the number of HCB. The opposite limit,  $\frac{s}{t} \rightarrow \infty$  (star geometry), has been shown recently to feature a real BEC where the occupation in the ground state scales as  $L\rho(1 - \rho + 1/L)$  with  $\rho = N/L$  [11].

In order to construct a full analytical solution, we introduce a mapping from the wheel Eq. (1) to a ladder geometry of HCB with periodic boundary conditions (see Fig. 1b). The overall solution strategy is sketched schematically in Fig. 2. The crucial step is to identify the central Hilbert space of the HCB wheel with the subspace of the single-particle momentum states  $|N_{\odot,k=0}\rangle_\odot$  on the inner ring of the ladder (enforcing occupations  $N_{\odot,k=0} \equiv N_\odot \leq 1$ ). The projector  $\hat{\Pi}_\odot$  to this subspace allows us to construct a solution on the expanded Hilbert space of the ladder geometry and eventually project down. Thereby, the long-range coupled wheel Hamiltonian can be mapped to an only next-nearest-neighbor (NNN) coupled ladder Hamiltonian  $\hat{H}_{\text{lad}}$ :

$$\hat{H} = \hat{\Pi}_\odot \hat{H}_{\text{lad}} \hat{\Pi}_\odot. \quad (2)$$

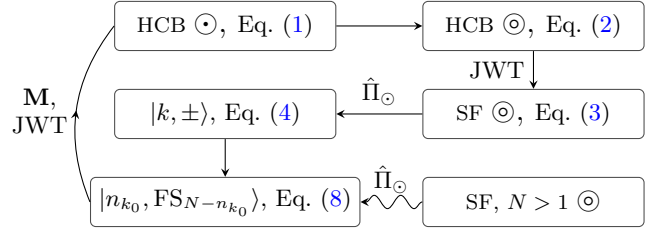


FIG. 2. Solution strategy for Eq. (1). The HCB wheel  $\odot$  is transformed to a ladder  $\ominus$ , which is then mapped to a ladder of spinless SF via a JWT. From the ladder of SF, the single-particle spectrum  $|k, \pm\rangle$  and therefrom projected Slater determinants  $|n_{k_0}, \text{FS}_{N-n_{k_0}}\rangle$  are constructed, utilizing the projector to the  $N_\odot \leq 1$  subspace,  $\hat{\Pi}_\odot$ . The constructed many-particle Slater determinants finally allow for the analytic solution of the full HCB wheel diagonalizing a  $4 \times 4$  matrix  $\mathbf{M}$ . Note that no closed solution of the SF ladder Hamiltonian is required (only its projected counterpart).

While the full details of the mapping can be found in [34], the most important observation is that a JWT of  $\hat{H}_{\text{lad}}$  introduces only local parity operators  $e^{i\pi\hat{n}_{\odot,j}}$ :

$$\hat{\Pi}_\odot \hat{H}_{\text{lad}} \hat{\Pi}_\odot = t \sum_j \hat{\Pi}_\odot \left( \hat{c}_j^\dagger e^{i\pi\hat{n}_{\odot,j}} \hat{c}_{j+1} + \text{h.c.} \right) \hat{\Pi}_\odot - \tilde{s} \sum_j \hat{\Pi}_\odot \left( e^{ik_0j} \hat{c}_j^\dagger \hat{c}_{\odot,j} + \text{h.c.} \right) \hat{\Pi}_\odot, \quad (3)$$

wherein  $\hat{c}_j^{(\dagger)}$  ( $\hat{c}_{\odot,j}^{(\dagger)}$ ) denotes the fermionic ladder operator on the  $j$ -th site of the outer (inner) ring and the single-site number operator on the inner ring is given by  $\hat{n}_{\odot,j} = \hat{c}_{\odot,j}^\dagger \hat{c}_{\odot,j}$ . We emphasize the appearance of a rescaled ring-to-center hopping amplitude  $\tilde{s} = s\sqrt{L}$ , that allows to connect to the known solutions when taking the thermodynamic limit  $L \rightarrow \infty$ . In fact, in the thermodynamic limit, the wheel immediately collapses to the star geometry whenever there is a fixed, finite ratio  $\frac{s}{t}$ , and the ground state is a true BEC. However, the question remains what happens for fixed ratios  $\frac{\tilde{s}}{t}$ . This matters for finite system sizes, as is the case for mesoscopic systems, in ultracold atomic gas experiments or Rydberg atoms [35]. In particular, we are interested in the impact of the extensive energy scale set by  $\tilde{s}$  on the formation and stability of the BEC, which requires a more in-depth analysis of the ground state of Eq. (3). Note that for now and in the following, we refer to the scaling of the ring-to-center hopping  $\tilde{s} = s\sqrt{L}$  as extensive in the system size.

It is instructive to first solve Eq. (3) for the single-particle eigenstates  $|k, \pm\rangle$ , fulfilling  $\langle e^{i\pi\hat{n}_{\odot,j}} \rangle \equiv 1$ :

$$|k, \pm\rangle = \begin{cases} c_k^\dagger |\emptyset\rangle & \text{if } k \neq k_0, \\ \psi_\pm \left( \hat{c}_k^\dagger + \Delta_\pm \hat{c}_{\odot,k=0}^\dagger \right) |\emptyset\rangle & \text{if } k = k_0. \end{cases} \quad (4)$$

Here,  $\hat{c}_{(\odot),k}^\dagger = \frac{1}{\sqrt{L}} \sum_{j=0}^{L-1} e^{-ikj} \hat{c}_{(\odot),j}^\dagger$  with  $\psi_{(k),\pm}$  being a nor-

malization constant and  $|\emptyset\rangle$  denotes the vacuum state. As shown in Fig. 1, the corresponding single-particle spectrum is identical to that of a tight-binding chain (i.e.,  $\varepsilon_k = 2t \cos k$ ) except for the  $k = k_0$  states whose single-particle energies are characterized by the splitting  $\Delta_{\pm} = \frac{\varepsilon_0}{2\tilde{s}} \pm \frac{\sqrt{\varepsilon_0^2 + 4\tilde{s}^2}}{|2\tilde{s}|}$ :

$$\varepsilon_{\pm} = \frac{1}{2} \left( \varepsilon_0 \pm \text{sgn}(\tilde{s}) \sqrt{\varepsilon_0^2 + 4\tilde{s}^2} \right) = \tilde{s} \Delta_{\pm}. \quad (5)$$

These  $k = k_0$  single-particle eigenstates Eq. (4) separate  $\propto |\tilde{s}| \propto \sqrt{L}$  from the remaining spectrum giving rise to a single-particle gap. Referring to Eq. (3), in the limit  $\frac{\tilde{s}}{t} \rightarrow \infty$ , the hopping on the outer ring can be neglected, and the same holds for the impact of the JWT on the overall eigenstate. Consequently, the single-particle gap can be expected to control the many-body spectrum, in this limit. Additionally, from  $\Delta_{\pm} \xrightarrow{\tilde{s}/t \rightarrow \infty} \pm 1$  we find that the corresponding wavefunction is characterized by a maximally mixing of the distinguished mode  $|k_0\rangle$  on the outer ring with the state  $|N_{\odot} = 1\rangle_{\odot}$  on the inner ring. This highly non-local wavefunction, generated from the extensive scaling of Eq. (5), already suggests the stability of the BEC under local perturbations on the outer ring.

In order to further elaborate on the extensive scaling property, we now return to the full solution of Eq. (1) with the complete derivation detailed in [34]. Here, the key observation is that Slater determinants constructed from single-particle states Eq. (4) with  $k \neq k_0$  are also eigenstates of  $\hat{H} = \hat{\Pi}_{\odot} \hat{H}_{\text{lad}} \hat{\Pi}_{\odot}$ :

$$\hat{\Pi}_{\odot} \hat{H}_{\text{lad}} \hat{\Pi}_{\odot} |\text{FS}_N\rangle = \left( \sum_{l=1}^N \varepsilon_{k_l} \right) \hat{\Pi}_{\odot} |\text{FS}_N\rangle, \quad (6)$$

where  $|\text{FS}_N\rangle = |k_1, \dots, k_N\rangle$  denotes a Slater determinant labeled by a set of  $N$  single-particle eigenstates with  $k_l \neq k_0$ . This observation can be understood by noting that the projected parity operator in Eq. (3) can be written in terms of the zero momentum density  $N_{\odot}$  on the inner ring

$$\hat{\Pi}_{\odot} e^{i\pi \hat{n}_{\odot,j}} \hat{\Pi}_{\odot} = \hat{1}_{\odot,j} - \frac{2}{L} \hat{c}_{\odot,k=0}^{\dagger} \hat{c}_{\odot,k=0}, \quad (7)$$

and thus  $\hat{\Pi}_{\odot} e^{i\pi \hat{n}_{\odot,j}} \hat{\Pi}_{\odot} |\text{FS}_N\rangle = |\text{FS}_N\rangle$ . Particle-number conservation of the wheel Hamiltonian then motivates to construct an ansatz for the  $N$ -particle eigenstates, superimposing all possible occupations of the  $k_0$  mode that belong to the same overall particle number sector

$$|\psi_N\rangle = \alpha_0 |\text{FS}_N\rangle + \left( \alpha_{1+} \hat{\psi}_{+}^{\dagger} + \alpha_{1-} \hat{\psi}_{-}^{\dagger} \right) |\text{FS}_{N-1}\rangle + \alpha_2 \hat{\psi}_{+}^{\dagger} \hat{\psi}_{-}^{\dagger} |\text{FS}_{N-2}\rangle, \quad (8)$$

with complex coefficients  $\alpha_{0,1\pm,2}$ . These states describe a superposition of either empty ( $\propto \alpha_0$ ) or doubly occupied ( $\propto \alpha_2$ )  $k_0$  states and highly non-local states  $\propto \alpha_{1\pm}$  in

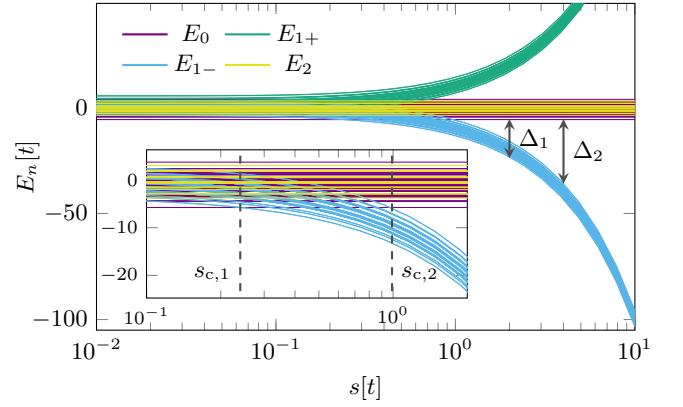


FIG. 3. Clustering of the many-particle eigenstates for a wheel composed of 10 lattice sites in the  $N = 4$  particle number sector as a function of the ring-to-center hopping  $s$ . Different colors correspond to the clustered energies generated from the different eigenvalues of Eq. (9). Indicated are also the two gaps defining the two critical ring-to-center hoppings  $s_{c,1}, s_{c,2}$ .

which the  $k_0$  mode on the outer ring is coupled to the  $|N_{\odot} = 1\rangle_{\odot}$  mode on the inner ring.

Using the orthogonality of different Slater determinants, it is a straightforward calculation to find that the general solution of the eigenvalue problem  $\hat{\Pi}_{\odot} \hat{H}_{\text{lad}} \hat{\Pi}_{\odot} |\text{FS}_N\rangle = E \hat{\Pi}_{\odot} |\text{FS}_N\rangle$  reduces to the diagonalization of a  $4 \times 4$  matrix. Fixing a Slater determinant  $|\text{FS}_N\rangle$  and two modes  $k', k'' \neq k_0$  so that  $\hat{c}_{k'} |\text{FS}_N\rangle = |\text{FS}_{N-1}\rangle$  as well as  $\hat{c}_{k''} \hat{c}_{k'} |\text{FS}_N\rangle = |\text{FS}_{N-2}\rangle$ , and labeling the 4 basis states by their possible occupations of the  $k = k_0$  mode  $n_{k_0} = 0, 1_{\pm}, 2$ , the resulting eigenvalue problem is of the form

$$\begin{pmatrix} h_0 & & & \\ & h_1 & & \\ & & & \\ & & & h_2 \end{pmatrix} \begin{pmatrix} \alpha_0 \\ \alpha_{1+} \\ \alpha_{1-} \\ \alpha_2 \end{pmatrix} = E \begin{pmatrix} \alpha_0 \\ \alpha_{1+} \\ \alpha_{1-} \\ \alpha_2 \end{pmatrix} \quad (9)$$

with  $h_0 = \langle 0 | \hat{H}_{\text{lad}} | 0 \rangle$ ,  $h_1 = \langle 1_{\mu} | \hat{H}_{\text{lad}} | 1_{\mu'} \rangle$  for  $\mu, \mu' \in \{+, -\}$ , and  $h_2 = \langle 2 | \hat{H}_{\text{lad}} | 2 \rangle$ . Note the block-diagonal structure that reflects the different  $k = k_0$  parities, i.e.,

$$e^{i\pi \hat{n}_{k_0}} |n_{k_0}\rangle = \begin{cases} |n_{k_0}\rangle, & \text{if } n_{k_0} = 0, 2, \\ -|n_{k_0}\rangle, & \text{if } n_{k_0} = 1_{+}, 1_{-}. \end{cases} \quad (10)$$

We emphasize the existence of a hidden  $\mathbb{Z}_2$  symmetry of the many-body eigenstates. This symmetry is an immediate consequence of the modulation of the hopping to the center site, i.e., it characterizes the  $k_0$ -occupation. Furthermore, condensation requires a breaking of particle number conservation on the outer ring, which is possible only in the  $n_{k_0} = 1_{\pm}$  subspace. Thus, an odd  $\mathbb{Z}_2$  symmetry of the ground state signals the formation of a BEC.

Upon solving Eq. (9), a special structure of the many-body spectrum appears that is characterized by a clustering of eigenstates belonging to the same  $k_0$ -parity sector, which is exemplified in Fig. 3. Therefrom, for a given filling fraction  $\rho = N/L$  we can extract the scaling of two critical parameters separating the low-lying odd-parity cluster (blue in Fig. 3), which hosts the BEC ground state, from the remaining eigenstates. In what follows we set  $t \equiv 1$  as unit of energy. The first critical hopping  $\tilde{s}_{c,1}$  and gap  $\Delta_1$  arise once the clustered odd-parity eigenstates constitute the overall ground state, indicating the condensation of bosons into the  $k_0$  mode (abbreviating  $X_\rho = \frac{\sin(\pi\rho)}{\pi}$ ):

$$\tilde{s}_{c,1} = \sqrt{8X_\rho}, \quad (11)$$

$$\Delta_1 = -(1 + 2X_\rho) + \sqrt{(1 - 2X_\rho)^2 + \tilde{s}^2} \quad (12)$$

The second critical hopping is defined by the complete separation of the odd-parity cluster from the even-parity many-particle eigenstates:

$$\tilde{s}_{c,2} = 4L\sqrt{X_\rho^2 + \mathcal{O}(L^{-1})}, \quad (13)$$

$$\Delta_2 = -4LX_\rho - (1 - 2X_\rho) + \sqrt{(1 + 2X_\rho)^2 + \tilde{s}^2}. \quad (14)$$

Note that  $\tilde{s} > \tilde{s}_{c,2}$  implies that scattering between states with even and odd  $k_0$  parity, caused by external perturbations, can only occur if the energy barrier  $\Delta_2$  can be overcome.

*Interactions on the outer ring.*— The analytical solution and, in particular, the property of BEC ground states exhibiting odd  $k = k_0$  parity allows to draw some striking conclusions on the stability of the BEC in the presence of local perturbations on the outer ring. Adding interactions acting on a finite subset of outer ring sites only, we note that in general the single-particle description breaks down in favor of a Luttinger liquid [36–39]. Therefore, interactions generically couple the two parity sectors in the  $k_0$  subspace and one might expect a breaking of the  $\mathbb{Z}_2$  symmetry. However, mixing of the  $k_0$  parity sectors caused by local interactions connecting  $d$  neighboring sites on the outer ring is of the order of  $\sim \frac{Vd}{\tilde{s}}$  where  $V$  is the largest interaction strength. The consequence is that increasing the number of lattice sites, i.e., the center site's coordination number,  $\mathbb{Z}_2$  symmetry of the  $k_0$  modes is approximately restored, stabilizing BEC in the presence of interactions on the outer ring.

We numerically checked the robustness of the BEC in the thermodynamic limit for  $k_0 = 0$  and finite values of the ring-to-center hopping. To this end, we calculated the ground-state occupation  $n_{k_0}(s, L)$  of the  $k_0 = 0$  mode [1, 40] using DMRG. Normalizing with respect to the upper bound on the condensate occupation  $n_{\max}(L) = L\rho(1 - \rho + 1/L)$  [11], we extrapolated the condensate fraction into the thermodynamic limit  $n_{k_0}(s)/n_{\max} = \lim_{L \rightarrow \infty} \frac{n_{k_0}(s, L)}{n_{\max}(L)}$  (see [34] for the details).

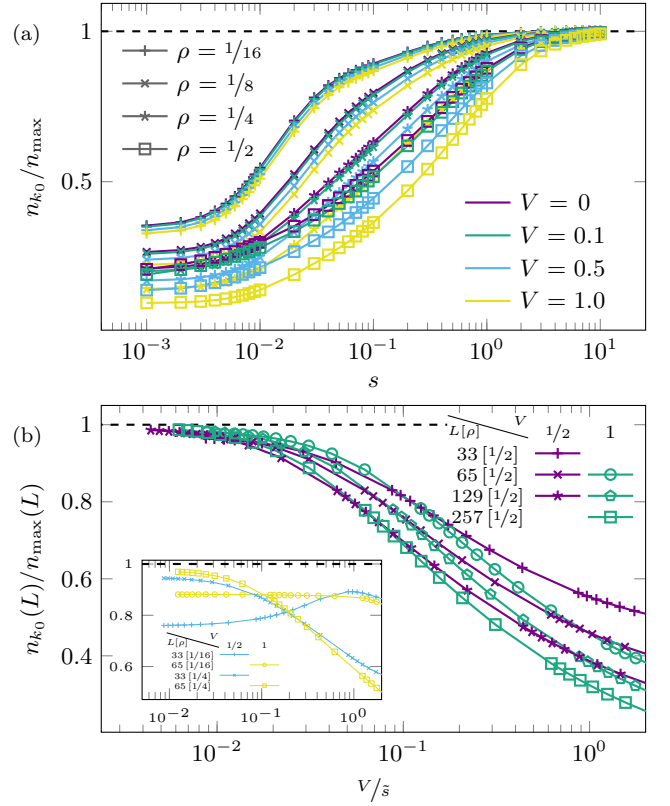


FIG. 4. (a) Ground-state BEC condensate fraction  $n(s)$  normalized to the maximally possible value  $n_{\max}$  [11] and extrapolated to the thermodynamic limit. (b) Asymptotically the normalized condensate fraction for a fixed number of lattice sites is a function of the ratio  $V/\tilde{s}$ , only. Results are shown for different NN interaction strengths  $V$  and densities on the ring  $\rho$ . Note that for very small fillings  $\rho = 1/16$  (inset of (b)), there are significant deviations of the observed connection between the condensate fraction and the ratio  $V/\tilde{s}$ . This originates from the flat single-particle dispersion around  $k = \pi$  (see Fig. 1). Thereby, the complete separation of the odd-parity states (controlled by  $\Delta_2$ ) occurs already for small ring-to-center hoppings, mainly independent on the number of lattice sites.

The resulting extrapolations are shown in Fig. 4a for interaction strengths between  $V = 0$  and  $V = 1$  and particle densities between  $\rho = 1/16$  and  $1/2$ . Note that even though there is a renormalization of the overall condensate fraction, we always observe a finite condensate density in the thermodynamic limit, even for strong interactions and high particle densities. To further demonstrate the asymptotic robustness of the  $\mathbb{Z}_2$  symmetry protection, in Fig. 4b the dependency of the condensate fraction at finite system sizes and as a function of  $V/\tilde{s}$  is shown. We also observe the behavior expected from our previous analysis, namely that the condensate occupation dominantly depends on the system size and the ratio between the interaction and the extensively scaling renormalized ring-to-center hopping  $\tilde{s} = s\sqrt{L}$ . In accordance to the scaling of  $\Delta_2$ , the maximally possible condensation is



reached if  $\tilde{s} \sim L$ . We emphasize that these relations can be translated to experimental realizations to determine the necessary coordination number, i.e., number of sites on the ring, to detect BEC in the presence of interactions.

*Conclusion.*— We introduced a solution strategy for models on a wheel with  $k_0$  modulated ring-to-center hopping  $s_j = se^{ik_0j}$ , which we applied to a system of HCB [9–12]. Our central finding is the protection of a BEC by a  $\mathbb{Z}_2$  symmetry emerging from the model-specific modulation of the hopping to the center site. We traced back this remarkable feature to an extensively scaling separation  $\propto s\sqrt{L}$  of the  $k = k_0$  single-particle modes, generated from the extensive coordination of the center with the ring sites. This scaling renders the BEC robust against local perturbations on the ring. We demonstrated this feature numerically by calculating the HCB  $k_0$ -condensate fraction of the ground state in the presence of NN interactions and for various particle number densities. Our calculations clearly show the protection of BEC where the condensate fraction is controlled by the ratio  $\frac{V}{s\sqrt{L}}$  and approaches the maximally possible value [11], even in the presence of strong interactions.

Our findings imply important consequences for both experimental and theoretical realizations of wheel geometries in general. First of all, a particular single-particle mode can be gapped out by a proper modulation of the ring-to-center hopping, allowing the general protection of ordered phases that are characterized by a certain wave vector. We believe that such a modulation of the ring-to-center hopping provides an experimentally feasible approach to realize exotic, finite-momentum BEC in the framework of ultracold or Rydberg atoms [28–31, 35, 41, 42]. Second, there is a many-body gap separating the BEC-carrying states from the remaining spectrum  $\sim s\sqrt{L}$ , i.e., large gaps can be realized by increasing the coordination number of the center site. The resulting robustness against interactions on the ring can be exploited to increase critical temperatures for phase transitions into otherwise highly fragile quantum phases. Possible applications are mesoscopic setups where a conducting center site may be contacted to one-dimensional ring geometries via tunnel contacts, allowing the stabilization of ordered states on the ring against perturbations. Such a scaling could also be exploited to increase the stability of superconducting qubits by means of an all-to-all-coupling of a set of noisy stabilizer qubits to a central qubit [43]. Moreover, we believe that the wheel-to-ladder mapping could prove useful in the analysis of hidden fermions [44]. Further interesting questions are the incorporation of disorder on both the ring and center site, as well as the effect of (artificial) gauge fields and a rescaled ring-to-center hopping  $s \rightarrow \frac{s}{\sqrt{L}}$  with regard to the crossover from one to an infinite number of dimensions.

*Acknowledgment.*— We thank F. Grusdt and U. Schollwöck for carefully reading the manuscript. Furthermore, we thank M. Bramberger and M. Grundner for very fruitful discussions. TK acknowledges financial support by the ERC Starting Grant from the European Union’s Horizon 2020 research and innovation program under grant agreement number 758935. FAP acknowledges funding by the Deutsche Forschungsgemeinschaft (DFG, German Research Foundation) via Research Unit FOR 2414 under project number 277974659. RHW, FAP and SP acknowledge support from the Munich Center for Quantum Science and Technology. The authors gratefully acknowledge the funding of this project by computing time provided by the Paderborn Center for Parallel Computing (PC<sup>2</sup>).

- 
- [1] O. Penrose and L. Onsager, *Phys. Rev.* **104**, 576 (1956).
  - [2] M. H. Anderson, J. R. Ensher, M. R. Matthews, C. E. Wieman, and E. A. Cornell, *Science* **269**, 198 (1995).
  - [3] D. Jaksch, C. Bruder, J. I. Cirac, C. W. Gardiner, and P. Zoller, *Phys. Rev. Lett.* **81**, 3108 (1998).
  - [4] I. Bloch, J. Dalibard, and W. Zwerger, *Rev. Mod. Phys.* **80**, 885 (2008).
  - [5] F. Dalfovo, S. Giorgini, L. P. Pitaevskii, and S. Stringari, *Rev. Mod. Phys.* **71**, 463 (1999).
  - [6] T. Giamarchi, C. Rüegg, and O. Tchernyshyov, *Nature Physics* **4**, 198 (2008).
  - [7] Y. N. M. de Escobar, P. G. Mickelson, M. Yan, B. J. Desalvo, S. B. Nagel, and T. C. Killian, *Phys. Rev. Lett.* **103**, 200402 (2009).
  - [8] S. Kraft, F. Vogt, O. Appel, F. Riehle, and U. Sterr, *Phys. Rev. Lett.* **103**, 130401 (2009).
  - [9] P. G. J. van Dongen, J. A. Vergés, and D. Vollhardt, *Zeitschrift für Physik B Condensed Matter* **84**, 383 (1991).
  - [10] E. J. G. Vidal, R. P. A. Lima, and M. L. Lyra, *Phys. Rev. E* **83**, 061137 (2011).
  - [11] F. Tennie, V. Vedral, and C. Schilling, *Phys. Rev. B* **96**, 064502 (2017).
  - [12] M. Máté, Ö. Legeza, R. Schilling, M. Yousif, and C. Schilling, *Communications Physics* **4**, 29 (2021).
  - [13] K. G. Wilson, *Rev. Mod. Phys.* **47**, 773 (1975).
  - [14] A. Georges, G. Kotliar, W. Krauth, and M. J. Rozenberg, *Rev. Mod. Phys.* **68**, 13 (1996).
  - [15] J. K. Freericks, V. M. Turkowski, and V. Zlatić, *Phys. Rev. Lett.* **97**, 266408 (2006).
  - [16] M. Eckstein and P. Werner, *Phys. Rev. B* **88**, 075135 (2013).
  - [17] H. Aoki, N. Tsuji, M. Eckstein, M. Kollar, T. Oka, and P. Werner, *Rev. Mod. Phys.* **86**, 779 (2014).
  - [18] P. Seth, I. Krivenko, M. Ferrero, and O. Parcollet, *Computer Physics Communications* **200**, 274 (2016).
  - [19] Gaudin, M., *J. Phys. France* **37**, 1087 (1976).
  - [20] N. V. Prokof and P. C. E. Stamp, *Rep. Prog. Phys.* **63**, 669 (2000).
  - [21] J. von Delft and D. Ralph, *Physics Reports* **345**, 61 (2001).

- [22] J. M. Taylor, A. Imamoglu, and M. D. Lukin, *Phys. Rev. Lett.* **91**, 246802 (2003).
- [23] J. Dukelsky, S. Pittel, and G. Sierra, *Rev. Mod. Phys.* **76**, 643 (2004).
- [24] T. Villazon, A. Chandran, and P. W. Claeys, *Phys. Rev. Research* **2** (2020).
- [25] Y. Ashida, T. Shi, R. Schmidt, H. R. Sadeghpour, J. I. Cirac, and E. Demler, *Phys. Rev. Lett.* **123**, 183001 (2019).
- [26] U. Schollwöck, *Rev. Mod. Phys.* **77**, 259 (2005).
- [27] U. Schollwöck, *Annals of Physics* **326**, 96 (2011), January 2011 Special Issue.
- [28] L.-K. Lim, C. M. Smith, and A. Hemmerich, *Phys. Rev. Lett.* **100**, 130402 (2008).
- [29] J. Hick, F. Sauli, A. Kreisel, and P. Kopietz, *The European Physical Journal B* **78**, 429 (2010).
- [30] M. Di Liberto, O. Tieleman, V. Branchina, and C. M. Smith, *Phys. Rev. A* **84**, 013607 (2011).
- [31] Y.-J. Lin, K. Jiménez-García, and I. B. Spielman, *Nature* **471**, 83 (2011).
- [32] E. H. Lieb and W. Liniger, *Phys. Rev.* **130**, 1605 (1963).
- [33] E. H. Lieb, *Phys. Rev.* **130**, 1616 (1963).
- [34] S. S. Material, Link will be added.
- [35] M. T. Eiles, A. Eisfeld, and J. M. Rost, *arXiv* (2021).
- [36] J. M. Luttinger, *J. Math. Phys.* **4**, 1154 (1963).
- [37] F. D. M. Haldane, *Journal of Physics C: Solid State Physics* **14**, 2585 (1981).
- [38] V. Meden and K. Schönhammer, *Phys. Rev. B* **46**, 15753 (1992).
- [39] H. J. Schulz, G. Cuniberti, and P. Pieri, in *Field Theories for Low-dimensional Condensed Matter Systems: Spin* edited by G. Morandi, P. Sodano, A. Tagliacozzo, and V. Tognetti (Springer Verlag, GmbH, 2000) pp. 9–82.
- [40] C. N. Yang, *Rev. Mod. Phys.* **34**, 694 (1962).
- [41] G. Summy and S. Wimberger, *Phys. Rev. A* **93**, 023638 (2016).
- [42] J. Manganonkar, C. Vishwakarma, S. S. Maurya, S. Sarkar, J. L. MacLennan, P. Dutta, and U. D. Rapol, *Journal of Physics B: Atomic, Molecular and Optical Physics* **53**, 235502 (2020).
- [43] P. Krantz, M. Kjaergaard, F. Yan, T. P. Orlando, S. Gustavsson, and W. D. Oliver, *Applied Physics Reviews* **6**, 021318 (2019).
- [44] S. Sakai, M. Civelli, and M. Imada, *Phys. Rev. Lett.* **116**, 057003 (2016).
- [45] S. R. White, *Phys. Rev. Lett.* **69**, 2863 (1992).
- [46] S. R. White, *Phys. Rev. B* **48**, 10345 (1993).
- [47] S. Paeckel and T. Köhler, “SYMMPs,” <https://www.symmps.eu>, accessed: 2021-04-01.

## Supplemental Materials

### WHEEL-TO-LADDER MAPPING

Here, we outline the mapping from the wheel geometry to the projected ladder in detail. The wheel Hamiltonian is given by

$$\hat{H} = -t \sum_{j=0}^{L-1} \left( \hat{h}_j^\dagger \hat{h}_{j+1} + \hat{h}_{j+1}^\dagger \hat{h}_j \right) - \sum_{j=0}^{L-1} \left( s_j \hat{h}_j^\dagger \hat{h}_\odot + \text{h.c.} \right), \quad (\text{S1})$$

with  $\hat{h}_j^{(\dagger)}$  ( $\hat{h}_\odot^{(\dagger)}$ ) describing hardcore bosonic degrees of freedom located on the outer ring (center site) and  $s_j = e^{ik_0 j}$  with  $k_0 = \frac{2\pi}{L}n$  ( $n \in \mathbb{Z}$ ) a reciprocal lattice vector. We consider periodic boundary conditions on the outer ring, i.e.,  $\hat{h}_L^{(\dagger)} = \hat{h}_0^{(\dagger)}$ . The model is defined on the tensor product Hilbert space  $\mathcal{H}_{L+1} = \mathcal{H}_2^{\otimes L} \otimes \mathcal{H}_\odot$ , where  $\mathcal{H}_2(\mathcal{H}_\odot)$  is the single-particle Hilbert space of a hardcore boson on the outer ring (center site). We define an enlarged Hilbert space of two concentric rings, where the Hilbert space of the inner ring is a copy of the Hilbert space of the outer ring.

$$\begin{aligned} \mathcal{H}_{L+1} &= \mathcal{H}_L \otimes \mathcal{H}_\odot = \mathcal{H}_2^{\otimes L} \otimes \mathcal{H}_2 \\ &\downarrow \\ \mathcal{H}_{\text{lad},L} &= \mathcal{H}_L \otimes \mathcal{H}_{\odot,L} = \mathcal{H}_2^{\otimes L} \otimes \mathcal{H}_2^{\otimes L} \end{aligned}$$

To describe hopping to the inner ring, we introduce  $\hat{h}_{\odot,j}^{(\dagger)}$  as the corresponding ladder operators acting on the sites of the inner ring. Note that sites with the same index on the inner and outer ring can be aligned vertically, yielding a ladder geometry. We introduce the second quantization basis for the inner ring

$$|n_{\odot,1}, n_{\odot,2}, \dots, n_{\odot,L}\rangle_\odot \in \mathcal{H}_{\odot,L}$$

as well as the vacuum state  $|\emptyset\rangle_\odot \in \mathcal{H}_{\odot,L}$ .

In order to represent the same physical situation as the wheel system, the total occupation of all sites on the inner ring must be either zero or one. Furthermore, we enforce the allowed states in  $\mathcal{H}_{\odot,L}$  to transform under rotations of

the inner ring, which is an a priori constraint so far, but will turn out to be very useful in the forthcoming discussion. We introduce  $\tilde{\mathcal{H}}_\odot$  by the set of states  $|\omega\rangle_\odot$  that meet these constraints

$$\tilde{\mathcal{H}}_\odot = \text{span} \{ |\omega\rangle_\odot \in \mathcal{H}_{\odot,L} \}.$$

On this subspace of  $\mathcal{H}_{\odot,L}$ , we then must have

$$\begin{aligned} \odot \langle \omega | \hat{N}_\odot | \omega \rangle_\odot &= \sum_j \odot \langle \omega | n_{\odot,j} | \omega \rangle_\odot = 0, 1 \\ \odot \langle \omega | [\hat{R}_\odot]^n | \omega \rangle_\odot &= e^{iq} \odot \langle \omega | [\hat{R}_\odot]^{n-1} | \omega \rangle_\odot, \quad q = \frac{2\pi}{L}m, \quad m \in \mathbb{Z} \end{aligned} \quad (\text{S2})$$

where  $n = 0, 1, \dots, L-1$  and  $\hat{R}_\odot$  applies a rotation to the inner ring:

$$\begin{aligned} \hat{R}_\odot : \mathcal{H}_{\odot,L} &\longrightarrow \mathcal{H}_{\odot,L} \\ |n_{\odot,1}, \dots, n_{\odot,L}\rangle_\odot &\longmapsto |n_{\odot,2}, \dots, n_{\odot,1}\rangle_\odot, \end{aligned}$$

and addition in the site indices is performed modulo  $L$ . The allowed states satisfying the above constraints are given by

$$|\omega = 0\rangle_\odot = |\emptyset\rangle_\odot \quad \text{and} \quad |\omega = 1\rangle_\odot = \frac{1}{\sqrt{L}} \sum_n e^{iqn} [\hat{R}_\odot]^n \hat{h}_{\odot,j}^\dagger |\emptyset\rangle_\odot, \quad (\text{S3})$$

for any  $j \in \{1, \dots, L\}$ .

Let us from now on identify  $|0\rangle_\odot$  ( $|1\rangle_\odot$ ) with the empty (occupied) inner site of the wheel. Having introduced the allowed states, we construct a Hamiltonian exhibiting the same matrix elements in  $\mathcal{P} = \mathcal{H}_L \otimes \tilde{\mathcal{H}}_\odot$  as Eq. (S1) in  $\mathcal{H}_{L+1}$ :

$$\hat{L}_\odot \equiv \underbrace{-t \sum_{j=0}^{L-1} \left( \hat{h}_j^\dagger \hat{h}_{j+1} + \text{h.c.} \right)}_{\hat{L}_{\odot,t}} - \sum_{j=0}^{L-1} \left( s_j \hat{h}_j^\dagger \hat{\omega}_\odot + \text{h.c.} \right).$$

Here, we defined operators  $\hat{\omega}_\odot = |0\rangle_\odot \langle 1|_\odot$  and  $\hat{\omega}_\odot^\dagger = |1\rangle_\odot \langle 0|_\odot$  via their action on  $|1\rangle_\odot$  and  $|0\rangle_\odot$ , respectively.

In order to obtain a representation of  $\hat{L}_\odot$  in  $\mathcal{P}$  we write

$$\hat{\omega}_\odot^{(\dagger)} |\emptyset\rangle = \frac{1}{\sqrt{L}} \sum_l e^{-iq_l} \hat{h}_{\odot,l}^{(\dagger)} |\emptyset\rangle, \quad (\text{S4})$$

where  $\hat{h}_{\odot,l}^{(\dagger)}$  acts on the  $l$ -th site of the inner ring, as well as a projector that projects to  $\mathcal{F}_{\odot,1} \subset \mathcal{H}_{\odot,L}$ , i.e., the Fock space spanned by empty and singly-occupied states on the inner ring:

$$\hat{P}_\odot = \prod_j \hat{n}_{\odot,j}^e + \sum_j \hat{n}_{\odot,j} \prod_{k \neq j} \hat{n}_{\odot,k}^e, \quad (\text{S5})$$

with  $\hat{n}_{\odot,j}^e = \hat{1}_{\odot,j} - \hat{n}_{\odot,j}$  and  $\hat{n}_{\odot,j} = \hat{h}_{\odot,j}^\dagger \hat{h}_{\odot,j}$ . Since  $\hat{P}_\odot^\dagger = \hat{P}_\odot$  and  $(\hat{P}_\odot)^2 = \hat{P}_\odot$ ,  $\hat{P}_\odot$  indeed is a projector. Rewriting  $\hat{\omega}_\odot$  and projecting down to  $\mathcal{F}_{\odot,1}$ , we obtain

$$\begin{aligned} \hat{H}_{\text{proj}} &= \hat{P}_\odot \hat{L}_\odot \hat{P}_\odot = \hat{P}_\odot \hat{L}_{\odot,t} \hat{P}_\odot + \frac{s}{\sqrt{L}} \sum_{j,l} \hat{P}_\odot \left( e^{ik_0 j} e^{-iq_l} \hat{h}_j^\dagger \hat{h}_{\odot,l} + \text{h.c.} \right) \hat{P}_\odot \\ &= \hat{P}_\odot \hat{L}_{\odot,t} \hat{P}_\odot + \frac{s}{\sqrt{L}} \sum_l e^{-iq_l} \hat{P}_\odot \left[ \hat{R}_\odot^\dagger \right]^l \left( \sum_j e^{ik_0 j} \hat{h}_j^\dagger \hat{h}_{\odot,j} \right) \left[ \hat{R}_\odot \right]^l \hat{P}_\odot + \text{h.c.} \\ &= \hat{P}_\odot \hat{L}_{\odot,t} \hat{P}_\odot + \frac{s}{\sqrt{L}} \sum_l \sum_{k,k'} |k\rangle_\odot \langle k| e^{-i(q+k-k')l} \hat{P}_\odot \left( \sum_j e^{ik_0 j} \hat{h}_j^\dagger \hat{h}_{\odot,j} \right) \hat{P}_\odot |k'\rangle_\odot \langle k'| + \text{h.c.} \\ &= \hat{P}_\odot \hat{L}_{\odot,t} \hat{P}_\odot + s\sqrt{L} \sum_k |k\rangle_\odot \langle k| \hat{P}_\odot \left( \sum_j e^{ik_0 j} \hat{h}_j^\dagger \hat{h}_{\odot,j} \right) \hat{P}_\odot |k+q\rangle_\odot \langle k+q| + \text{h.c.} \end{aligned} \quad (\text{S6})$$

which now acts on  $\mathcal{H}_L \otimes \mathcal{F}_{\odot,1}$ . We introduced  $|k\rangle_{\odot}$ , the eigenstates of  $\hat{R}_{\odot}$ , labeled by the respective rotation angle  $k = \frac{2\pi}{L}n$  with  $n \in \{0, \dots, L-1\}$  so that  $\hat{R}_{\odot} |k\rangle_{\odot} = e^{ik} |k\rangle_{\odot}$ . In the single-particle subspace on the inner ring, these states are given by

$$|k\rangle_{\odot} = \frac{1}{\sqrt{L}} \sum_{j=0}^{L-1} e^{ikj} \hat{h}_{\odot,j}^{\dagger} |\emptyset\rangle_{\odot} . \quad (\text{S7})$$

In order to obtain a representation that is block-diagonal in the  $|k\rangle_{\odot}$ -basis we choose  $q = 0$ :

$$\hat{H}_{\text{proj}} = \hat{P}_{\odot} \hat{H}_{\text{lad}} \hat{P}_{\odot} , \quad \hat{H}_{\text{lad}} = -t \sum_j \left( \hat{h}_j^{\dagger} \hat{h}_{j+1} + \text{h.c.} \right) - \tilde{s} \sum_j \left( e^{ik_0 j} \hat{h}_j^{\dagger} \hat{h}_{\odot,j} + \text{h.c.} \right) . \quad (\text{S8})$$

We note that  $\hat{H}_{\text{proj}}$  has long-ranged hoppings while  $\hat{H}_{\text{lad}}$  does not. Importantly, the eigenstates of  $\hat{R}_{\odot}$  are eigenstates of  $\hat{H}_{\text{proj}}$  due to  $[\hat{H}_{\text{proj}}, \hat{R}_{\odot}] = 0$ , while this is not the case for  $\hat{H}_{\text{lad}}$ , since  $[\hat{R}_{\odot}, \hat{H}_{\text{lad}}] \neq 0$ . Since  $[\hat{N}_{\odot}, \hat{R}_{\odot}] = 0$  holds, with  $\hat{N}_{\odot}$  being the total particle number on the inner ring, we may set up the simultaneous eigenstates and group them by their corresponding eigenvalues of  $\hat{R}_{\odot}$ :

$$N_{\odot} = 0 \Rightarrow |N_{\odot} = 0, k = 0\rangle_{\odot} \text{ is uniquely specified in the subspace with } \hat{N}_{\odot} = 0, \quad (\text{S9})$$

$$N_{\odot} = 1 \Rightarrow |N_{\odot} = 1, k = \frac{2\pi}{L}n\rangle_{\odot} \text{ are } L \text{ different states in the subspace } \hat{N}_{\odot} = 1. \quad (\text{S10})$$

They span the Fock space  $\mathcal{F}_{\odot,1}$ . The allowed states Eq. (S3) are obtained by taking only the states with  $k = 0$  in Eq. (S7). For brevity, we define  $|\emptyset\rangle_{\odot} = |N_{\odot} = 0, k = 0\rangle_{\odot}$  and  $|k = 0\rangle_{\odot} = |N_{\odot} = 1, k = 0\rangle_{\odot}$ . Now, let  $\hat{\Pi}_{\odot} = |\emptyset\rangle_{\odot} \langle \emptyset| + |k = 0\rangle_{\odot} \langle k = 0|$  be the projector into the  $k = 0$  subspace on the inner ring. We can thus write the initial Hamiltonian Eq. (S1), mapped to the ladder geometry as

$$\hat{H} \equiv \hat{\Pi}_{\odot} \hat{H}_{\text{proj}} \hat{\Pi}_{\odot} = \hat{\Pi}_{\odot} \hat{P}_{\odot} \hat{H}_{\text{lad}} \hat{P}_{\odot} \hat{\Pi}_{\odot} = \hat{\Pi}_{\odot} \hat{H}_{\text{lad}} \hat{\Pi}_{\odot} . \quad (\text{S11})$$

This establishes the mapping between the eigenstates of  $\hat{\Pi}_{\odot} \hat{H}_{\text{lad}} \hat{\Pi}_{\odot}$ , which will be computed explicitly later on, and the desired eigenstates of Eq. (S1), i.e., we need to find the many-particle eigenstates of Eq. (S6) projected into the  $k = 0$  sector. For that purpose, we employ a Jordan-Wigner transformation expressing the hardcore bosonic ladder operators in terms of fermionic ones. Implementing the ladder geometry via the mappings  $\hat{h}_j^{(\dagger)} \mapsto \hat{h}_{2j}^{(\dagger)}$  and  $\hat{h}_{\odot,j}^{(\dagger)} \mapsto \hat{h}_{2j+1}^{(\dagger)}$  yields the fermionic ladder operators

$$\hat{c}_j^{(\dagger)} = \prod_{k < j} e^{i\pi \hat{n}_k} \hat{h}_j^{(\dagger)} , \text{ with } j = 0, \dots, 2L-1. \quad (\text{S12})$$

After transforming the Hamiltonian, we reintroduce fermionic operators on the inner and outer ring via  $\hat{c}_{2j}^{(\dagger)} \mapsto \hat{c}_j^{(\dagger)}$  and  $\hat{c}_{2j+1}^{(\dagger)} \mapsto \hat{c}_{\odot,j}^{(\dagger)}$  and obtain

$$\hat{H}_{\text{lad}} = t \sum_j \left( \hat{c}_j^{\dagger} e^{i\pi \hat{n}_{\odot,j}} \hat{c}_{j+1} + \text{h.c.} \right) - \tilde{s} \sum_j \left( e^{ik_0 j} \hat{c}_j^{\dagger} \hat{c}_{\odot,j} + \text{h.c.} \right) . \quad (\text{S13})$$

## SOLUTION OF THE SINGLE-PARTICLE PROBLEM

In the single-particle subspace, the Jordan-Wigner transformed ladder Hamiltonian becomes

$$\hat{H}_{\text{lad}} = t \sum_j \left( \hat{c}_j^{\dagger} \hat{c}_{j+1} + \text{h.c.} \right) - \tilde{s} \sum_j \left( e^{ik_0 j} \hat{c}_j^{\dagger} \hat{c}_{\odot,j} + \text{h.c.} \right) . \quad (\text{S14})$$

It is instructive to explicitly construct the single-particle eigenstates subject to the projection into the  $q = 0$  subspace, where for brevity we introduce the decomposition  $\hat{H}_{\text{lad}} = \hat{H}_{\text{lad},t} + \hat{H}_{\text{lad},s}$ . We begin by considering the action of the



summands on rotational eigenstates  $|k\rangle_{(\odot)}$  on the outer (inner) ring:

$$\hat{H}_{\text{lad},t} |k\rangle |\emptyset\rangle_{\odot} = |k\rangle |\emptyset\rangle_{\odot} \quad \text{and} \quad \hat{H}_{\text{lad},t} |\emptyset\rangle |k\rangle_{\odot} = 0, \quad (\text{S15})$$

$$\hat{H}_{\text{lad},s} |k\rangle |\emptyset\rangle_{\odot} = \sum_{j,l} e^{-ik_0 j} \hat{c}_{\odot,j}^{\dagger} \hat{c}_j \frac{e^{ikl}}{\sqrt{L}} \hat{c}_l^{\dagger} |\emptyset\rangle |\emptyset\rangle_{\odot} = |\emptyset\rangle |k - k_0\rangle_{\odot}, \quad (\text{S16})$$

$$\hat{H}_{\text{lad},s} |\emptyset\rangle |k\rangle_{\odot} = \sum_{j,l} e^{ik_0 j} \hat{c}_j^{\dagger} \hat{c}_{\odot,j} \frac{e^{ikl}}{\sqrt{L}} \hat{c}_{\odot,l}^{\dagger} |\emptyset\rangle |\emptyset\rangle_{\odot} = |k + k_0\rangle |\emptyset\rangle_{\odot}. \quad (\text{S17})$$

For the projected eigenvalue equation this motivates the Ansatz  $\hat{\Pi}_{\odot} |\psi_k\rangle = |k\rangle |\emptyset\rangle_{\odot}$ ,

$$\hat{\Pi}_{\odot} \hat{H}_{\text{lad}} \hat{\Pi}_{\odot} |\psi_k\rangle = \hat{\Pi}_{\odot} (\epsilon_k |k\rangle |\emptyset\rangle_{\odot} - \tilde{s} |\emptyset\rangle |k - k_0\rangle_{\odot}) \quad (\text{S18})$$

$$= \epsilon_k |k\rangle |\emptyset\rangle_{\odot} - \tilde{s} \hat{\Pi}_{\odot} |\emptyset\rangle |k - k_0\rangle_{\odot}, \quad (\text{S19})$$

where  $\epsilon_k = 2t \cos(k)$  is the single-particle dispersion relation of non-interacting, spinless fermions. For  $k \neq k_0$ ,  $\hat{\Pi}_{\odot} |\psi_k\rangle$  indeed satisfies the eigenvalue equation. In order to determine the  $k = k_0$  single-particle eigenstates we make the ansatz  $\hat{\Pi}_{\odot} |\psi_{k_0}\rangle = \sum_{k'} c_{k'} |k'\rangle |\emptyset\rangle_{\odot} + \Delta |\emptyset\rangle |0\rangle_{\odot}$

$$\begin{aligned} \hat{\Pi}_{\odot} \hat{H}_{\text{lad}} \hat{\Pi}_{\odot} |\psi_k\rangle &= \left( \sum_{k'} \epsilon_{k'} c_{k'} |k'\rangle - \Delta \tilde{s} |k_0\rangle \right) |\emptyset\rangle_{\odot} - \tilde{s} c_{k_0} |\emptyset\rangle |0\rangle_{\odot} \\ &\stackrel{!}{=} \epsilon_{k_0} \left( \sum_{k'} c_{k'} |k'\rangle |\emptyset\rangle_{\odot} + \Delta |\emptyset\rangle |0\rangle_{\odot} \right) \end{aligned} \quad (\text{S20})$$

Setting  $c_{k'} = \delta_{k',k_0} c_{k_0}$  and choosing  $c_{k_0} = 1$ , we can solve for  $\Delta$

$$\begin{aligned} (\epsilon_{k_0} - \Delta \tilde{s}) |k_0\rangle |\emptyset\rangle_{\odot} - \tilde{s} |\emptyset\rangle |0\rangle_{\odot} &= \epsilon_{k_0} (|k_0\rangle |\emptyset\rangle_{\odot} + \Delta |\emptyset\rangle |0\rangle_{\odot}) \\ \rightarrow \Delta_{\pm} &= \frac{\epsilon_{k_0}}{2\tilde{s}} \pm \sqrt{\frac{\epsilon_{k_0}^2}{4\tilde{s}^2} + 1}, \end{aligned} \quad (\text{S21})$$

Thus, for  $k = k_0$ , there are two orthogonal single-particle eigenstates

$$|\psi_{k_0,\pm}\rangle = \psi_{k_0,\pm} \left( \hat{c}_{k_0}^{\dagger} + \Delta_{\pm} \hat{c}_{\odot,k=0}^{\dagger} \right) |\emptyset\rangle. \quad (\text{S22})$$

In this representation, projecting down the eigenstates into the zero-momentum sector on the inner ring is particularly easy:

$$|k, \pm\rangle = \hat{\Pi}_{\odot} |\psi_{k,\pm}\rangle = \begin{cases} \psi_k \hat{c}_k^{\dagger} |\emptyset\rangle & \text{if } k \neq k_0, \\ \psi_{\pm}^{\dagger} |\emptyset\rangle \equiv \psi_{\pm} \left( \hat{c}_k^{\dagger} + \Delta_{\pm} \hat{c}_{\odot,k=0}^{\dagger} \right) |\emptyset\rangle & \text{if } k = k_0. \end{cases} \quad (\text{S23})$$

Using Eq. (S11), the single-particle problem of the wheel Hamiltonian Eq. (S1) is thus solved by expanding the ladder problem in terms of the  $|\psi_{k,\mu}\rangle$  and projecting into the  $q = 0$  subspace

$$\begin{aligned} \hat{H} &\equiv \hat{\Pi}_{\odot} \sum_{k,k'} \sum_{\mu,\mu'=\pm} |\psi_{k,\mu}\rangle \langle \psi_{k,\mu} | \hat{\Pi}_{\odot} \hat{H}_{\text{lad}} \hat{\Pi}_{\odot} |\psi_{k',\mu'}\rangle \langle \psi_{k',\mu'} | \hat{\Pi}_{\odot} \\ &= \sum_{k \neq k_0} \epsilon_k |k\rangle \langle k| \otimes |\emptyset\rangle_{\odot} \langle \emptyset| + \sum_{\mu=\pm} \varepsilon_{\mu} |\psi_{k=k_0,\mu}\rangle \langle \psi_{k=k_0,\mu}|, \end{aligned} \quad (\text{S24})$$

where  $\varepsilon_{\pm} = \frac{1}{2} (\varepsilon_0 \pm \text{sgn}(\tilde{s}) \sqrt{\varepsilon_0^2 + 4\tilde{s}^2})$ . For later convenience, we also introduce ladder operators  $\hat{\psi}_{k,\mu}^{(\dagger)}$  annihilating (creating) single-particle modes  $|\psi_{k,\mu}\rangle$ . From Eq. (S22) it can be readily checked that they obey fermionic anticommutation relations

$$\left\{ \hat{\psi}_{k,\mu}^{(\dagger)}, \hat{\psi}_{k',\mu'}^{(\dagger)} \right\} = 0 \quad \text{and} \quad \left\{ \hat{\psi}_{k,\mu}, \hat{\psi}_{k',\mu'}^{\dagger} \right\} = \delta_{k,k'} \delta_{\mu,\mu'}. \quad (\text{S25})$$

## SOLUTION OF THE MANY-PARTICLE PROBLEM

The solution of the full many-particle problem Eq. (S1) is done with the help of Slater determinants constructed from the single-particle eigenstates Eq. (S23). Here, the important point is that all many-particle Slater determinants with either empty or doubly occupied  $k = k_0$  modes are already eigenstates of the projected ladder Eq. (S11) and thereby of the wheel Hamiltonian. In order to prove this observation, we define for a given set of  $N$  modes  $\mathbf{k}_N = (k_1, \dots, k_N)$  with  $k_l = \frac{2\pi}{L}n_l \neq k_0$  and  $0 \leq n_l < L$  projected Slater determinants of single-particle eigenstates of  $\hat{H}_{\text{lad}}$

$$|\mathbf{k}_N\rangle = |k_1, \dots, k_N\rangle = \hat{\Pi}_\odot |\psi_{k_1}, \dots, \psi_{k_N}\rangle = \hat{c}_{k_1}^\dagger \cdots \hat{c}_{k_N}^\dagger |\emptyset\rangle, \quad (\text{S26})$$

wherein we fixed the global phase by normal ordering the modes:  $k_1 < k_2 < \dots < k_N$ . Within this ordering, Slater determinants with modes  $|\psi_{k=k_0, \pm}\rangle$  occupied are always moved to the left and denoted by:

$$|n_+, n_-\rangle |\mathbf{k}_N\rangle = \left[ \hat{\psi}_{k_0, +}^\dagger \right]^{n_+} \left[ \hat{\psi}_{k_0, -}^\dagger \right]^{n_-} |\mathbf{k}_N\rangle. \quad (\text{S27})$$

Note that in the main text, we used a more condensed notation for the  $|\psi_{k=k_0, \pm}\rangle$  modes, labeling only the overall occupation via the abbreviations  $|0, 0\rangle \rightarrow |0\rangle$ ,  $|1, 0\rangle \rightarrow |1_+\rangle$ ,  $|0, 1\rangle \rightarrow |1_-\rangle$  and  $|1, 1\rangle \rightarrow |2\rangle$ . However, for clarity reasons, here we maintain the extended representation. Having setup this notation, we consider the action of the Jordan-Wigner-transformed wheel Hamiltonian in the projected ladder presentation on these Slater determinants

$$\begin{aligned} \hat{H} |n_+, n_-\rangle |\mathbf{k}_N\rangle &= \hat{\Pi}_\odot \hat{H}_{\text{lad}} \hat{\Pi}_\odot |n_+, n_-\rangle |\mathbf{k}_N\rangle \\ &= \hat{\Pi}_\odot \left( t \sum_{j=0}^{L-1} \left( \hat{c}_j^\dagger e^{i\pi \hat{n}_\odot, j} \hat{c}_{j+1} + \text{h.c.} \right) - \sum_{j=0}^{L-1} \left( \tilde{s}_j \hat{c}_j^\dagger \hat{c}_{\odot, j} + \text{h.c.} \right) \right) \hat{\Pi}_\odot |n_+, n_-\rangle |\mathbf{k}_N\rangle. \end{aligned} \quad (\text{S28})$$

In order to proceed, in the first sum we expand the operators acting on the inner ring in terms of rotations, i.e., perform a Fourier transformation (using  $k_n = \frac{2\pi}{L}n$ ) and apply the projection to the  $q = 0$  subspace

$$\hat{c}_{\odot, j}^\dagger = \frac{1}{\sqrt{L}} \sum_{n=0}^{L-1} e^{-ik_n j} \hat{c}_{\odot, k_n}^\dagger, \quad \hat{c}_{\odot, j} = \frac{1}{\sqrt{L}} \sum_{n=0}^{L-1} e^{ik_n j} \hat{c}_{\odot, k_n}, \quad (\text{S29})$$

$$\begin{aligned} \Rightarrow \hat{\Pi}_\odot e^{i\pi \hat{n}_\odot, j} \hat{\Pi}_\odot &= \hat{\Pi}_\odot (1 - 2\hat{n}_{\odot, j}) \hat{\Pi}_\odot = 1 - \hat{\Pi}_\odot \left( \frac{2}{L} \sum_{n, m=0}^{L-1} e^{-i(k_n - k_m)j} \hat{c}_{\odot, k_n}^\dagger \hat{c}_{\odot, k_m} \right) \hat{\Pi}_\odot \\ &= 1 - \frac{2}{L} \hat{c}_{\odot, k_n=0}^\dagger \hat{c}_{\odot, k_n=0} \equiv 1 - \frac{2}{L} \hat{n}_{\odot, k_n=0}. \end{aligned} \quad (\text{S30})$$

In a similar manner, we expand the second sum in terms of rotations of both the outer and inner ring yielding

$$\hat{H} |n_+, n_-\rangle |\mathbf{k}_N\rangle = \left( \underbrace{t \sum_{j=0}^{L-1} \left( \hat{c}_j^\dagger \hat{c}_{j+1} + \text{h.c.} \right)}_{\sum_{n=0}^{L-1} \varepsilon_{k_n} \hat{c}_{k_n}^\dagger \hat{c}_{k_n}} \left( 1 - \frac{2}{L} \hat{n}_{\odot, k=0} \right) - \left( \tilde{s}_j \hat{c}_{k=k_0}^\dagger \hat{c}_{\odot, k=0} + \text{h.c.} \right) \right) |n_+, n_-\rangle |\mathbf{k}_N\rangle. \quad (\text{S31})$$

Using  $\hat{c}_{k=k_0}^\dagger \hat{c}_{\odot, k=0} |0, 0\rangle |\mathbf{k}_N\rangle = 0$  as well as  $(1 - \frac{2}{L} \hat{n}_{\odot, k=0}) |0, 0\rangle |\mathbf{k}_N\rangle = |0, 0\rangle |\mathbf{k}_N\rangle$ , we immediately find that Slater determinants with empty  $k = k_0$  modes are eigenstates of  $\hat{H}$  with eigenvalues  $E(\mathbf{k}_N) = \sum_{l=1}^N \varepsilon_{k_l}$ .

Having found Eq. (S31) the solution strategy for the many-particle problem is straightforward. Employing total particle-number conservation, we decompose the many-particle Hilbert space into orthogonal subspaces  $\mathcal{H}_N$  with fixed total particle number  $N$ . Each  $N$ -particle subspace is then stratified into 4-dimensional subspaces  $\mathcal{H}_{k', k'', \mathbf{k}_{N-2}}$  that are parametrized by a set of  $N$  different modes  $\mathbf{k}_N = \mathbf{k}_{N-2} \cup \{k', k''\}$  with  $k_l, k', k'' \neq k_0$ , and we specified two distinct modes  $k', k''$ . A subspace  $\mathcal{H}_{k', k'', \mathbf{k}_{N-2}}$  is given by the linear hull of states

$$|\mathbf{k}_{N-2}, k', k''\rangle = \alpha_0 |\mathbf{k}_{N-2}, k', k''\rangle + \alpha_{1+} |1, 0\rangle |\mathbf{k}_{N-2}, k'\rangle + \alpha_{1-} |0, 1\rangle |\mathbf{k}_{N-2}, k'\rangle + \alpha_2 |1, 1\rangle |\mathbf{k}_{N-2}\rangle, \quad (\text{S32})$$

with complex coefficients  $\alpha_{0,1+,1-,2} \in \mathbb{C}$ . Using orthogonality of the Slater determinants, it can be checked that this stratification yields a complete decomposition of the  $N$ -particle Hilbert space by counting the dimensionalities. Varying the set of modes  $\mathbf{k}_{N-2} \cup \{k', k''\}$ , the number of orthogonal basis states is obtained from the right hand side of Eq. (S32) via

$$\dim \bigoplus_{\mathbf{k}_N, k', k''} \mathcal{H}_{k', k'', \mathbf{k}_{N-2}} = \binom{L-1}{N} + 2 \binom{L-1}{N-1} + \binom{L-1}{N-2} = \binom{L}{N} + \binom{L}{N-1} = \binom{L+1}{N} = \dim \mathcal{H}_N. \quad (\text{S33})$$

The last equality shows that indeed, the choosen parametrization generates a complete basis set for  $\mathcal{H}_N$ . It is also easy to see that  $\hat{\Pi}_{\odot} \hat{H}_{\text{lad}} \hat{\Pi}_{\odot}$  does not mix states belonging to different subspaces  $\mathcal{H}_{k', k'', \mathbf{k}_{N-2}}$  by noting that Eq. (S31) can only change the occupation of the  $k = k_0$  modes. Thus, we can solve the eigenvalue equation in each subspace separately, i.e., diagonalizing a  $4 \times 4$  matrix where, in the following, we abbreviate the Slater determinants suppressing the chosen set of  $k$ -values:

$$|0, 0\rangle |\mathbf{k}_{N-2}, k', k''\rangle \equiv |0, 0\rangle, \quad |1, 0\rangle |\mathbf{k}_{N-2}, k'\rangle \equiv |1, 0\rangle, \quad |0, 1\rangle |\mathbf{k}_{N-2}, k'\rangle \equiv |0, 1\rangle \quad \text{and} \quad |1, 1\rangle |\mathbf{k}_{N-2}\rangle \equiv |1, 1\rangle. \quad (\text{S34})$$

Using Eq. (S31) we immediately find

$$h_0 = \langle n_+, n_- | \hat{H} | 0, 0 \rangle = \delta_{n_+, 0} \delta_{n_-, 0} E(\mathbf{k}_N) \quad \text{and} \quad h_2 = \langle n_+, n_- | \hat{H} | 1, 1 \rangle = \delta_{n_+, 1} \delta_{n_-, 1} (E(\mathbf{k}_{N-2}) + \epsilon_{k_0}) \left(1 - \frac{2}{L}\right), \quad (\text{S35})$$

i.e., Slater determinants with empty or doubly occupied  $k = k_0$  mode are both eigenstates of  $\hat{H}$ . The remaining matrix elements evaluate to

$$\begin{aligned} \langle 1, 0 | \hat{H} | 1, 0 \rangle &= \frac{\Delta_+ (a\Delta_+ - 2\tilde{s}) + b}{1 + \Delta_+^2}, \\ \langle 0, 1 | \hat{H} | 0, 1 \rangle &= \frac{\Delta_- (a\Delta_- - 2\tilde{s}) + b}{1 + \Delta_-^2}, \\ \langle 1, 0 | \hat{H} | 0, 1 \rangle &= \frac{a\Delta_+ \Delta_- + \tilde{s}(\Delta_+ + \Delta_-) + b}{\sqrt{(1 + \Delta_+^2)(1 + \Delta_-^2)}} = \langle 0, 1 | \hat{H} | 1, 0 \rangle, \end{aligned} \quad (\text{S36})$$

with the definitions  $a = E(\mathbf{k}_{N-1}) \left(1 - \frac{2}{L}\right)$ ,  $b = \epsilon_{k_0} + E(\mathbf{k}_{N-1})$  as well as  $E(\mathbf{k}_{N-1}) = E(\mathbf{k}_N) - \epsilon_{k'}$ . Diagonalizing the  $2 \times 2$  matrix and setting  $t \equiv 1$  as unit of energy finally yields the desired eigenvalues

$$\begin{aligned} E_0(\mathbf{k}_{N-2}, k', k'') &= E(\mathbf{k}_N) \\ E_{1\pm}(\mathbf{k}_{N-2}, k') &= E(\mathbf{k}_{N-1}) \left(1 - \frac{1}{L}\right) + 1 \pm \sqrt{\left(\frac{E(\mathbf{k}_{N-1})}{L} + 1\right)^2 + \tilde{s}^2} \\ E_2(\mathbf{k}_N) &= (E(\mathbf{k}_{N-2}) + 2) \left(1 - \frac{2}{L}\right). \end{aligned} \quad (\text{S37})$$

These calculations imply a clustering of the many-particle eigenvalues as shown in Fig. 3 in the main text. For the set of all allowed modes  $\mathbf{k}_{N-2} \cup \{k', k''\}$  excluding  $k = k_0$ , each of the 4 energies consitutes a bulk of many-particle eigenvalues to the total spectrum with a bandwidth  $\sim E(\mathbf{k}_N)$ . Furthermore, for large system sizes  $L \gg 1$ , the level spacing in the bulk of the clustered many-particle eigenvalues scales as  $\sim \frac{2\pi}{L}$ . Importantly, the clustered eigenvalues behave differently, depending on the occupations of the  $k = k_0$  modes. For the case of empty or doubly occupied  $k = k_0$  modes, up to corrections  $\sim \frac{1}{L}$  the spectrum is given by the summed single-particle energies ( $E(\mathbf{k}_N)$  and  $(E(\mathbf{k}_{N-2}) + 2)$ ). If, however the  $k = k_0$  mode is singly occupied, we obtain a separation of the clustered many-particle eigenvalues  $\sim \pm |\tilde{s}|$ . We want to point out that in the latter case, the overall dependency of the many-particle eigenvalues on the ring-to-center coupling closely resembles that of single-particle dispersion relation of the underlying fermionic ladder Hamiltonian upon replacing  $\epsilon_k \rightarrow E(\mathbf{k}_{N-1})$ . This is not by accident but a result of the extensively scaling coordination number of the central site, restoring the single-particle character.

The previous discussion suggest the definition two energy gaps  $\Delta_1, \Delta_2$  characterizing the transition to the BEC phase as indicated in Fig. 3 in the main text. Note that as soon as  $\Delta_1 > 0$  the ground state is characterized by singly occupied  $k = k_0$  modes, i.e., an odd  $k = k_0$  parity that is separated from the clustered many-body states with

even  $k = k_0$  parity and therefore, empty or doubly occupied  $k = k_0$  modes. Thus,  $\Delta_1 > 0$  indicates a condensation of bosons into the  $k = k_0$  mode. However, only if  $\Delta_2 > 0$  there is a finite gap between the different parity symmetry sectors, otherwise the clusters with even and odd  $k = k_0$  parity are overlapping. Evaluating the gaps using Eq. (S37) in the limit  $L \gg 1$  and defining  $\rho = N/L$  yields

$$\begin{aligned}\Delta_1 &= -\left(1 + \frac{2\sin(\pi\rho)}{\pi}\right) + \sqrt{\left(1 - \frac{2\sin(\pi\rho)}{\pi}\right)^2 + \tilde{s}^2} \\ \Delta_2 &= -4L\frac{\sin(\pi\rho)}{\pi} - \left(1 - \frac{2\sin(\pi\rho)}{\pi}\right) + \sqrt{\left(1 + \frac{2\sin(\pi\rho)}{\pi}\right)^2 + \tilde{s}^2}\end{aligned}\quad (\text{S38})$$

and thus the critical ring-to-center hoppings are given by

$$s_{c,1} = \frac{2}{\sqrt{L}}\sqrt{\frac{2\sin(\pi\rho)}{\pi}} \quad \text{and} \quad s_{c,2} = 2\sqrt{L}\sqrt{\frac{\sin(\pi\rho)}{\pi} \left(\frac{4\sin(\pi\rho)}{\pi} + 2\frac{1 - \frac{2\sin(\pi\rho)}{\pi}}{L} - \frac{2}{L^2}\right)}. \quad (\text{S39})$$

## NUMERICAL DETAILS

### General remarks

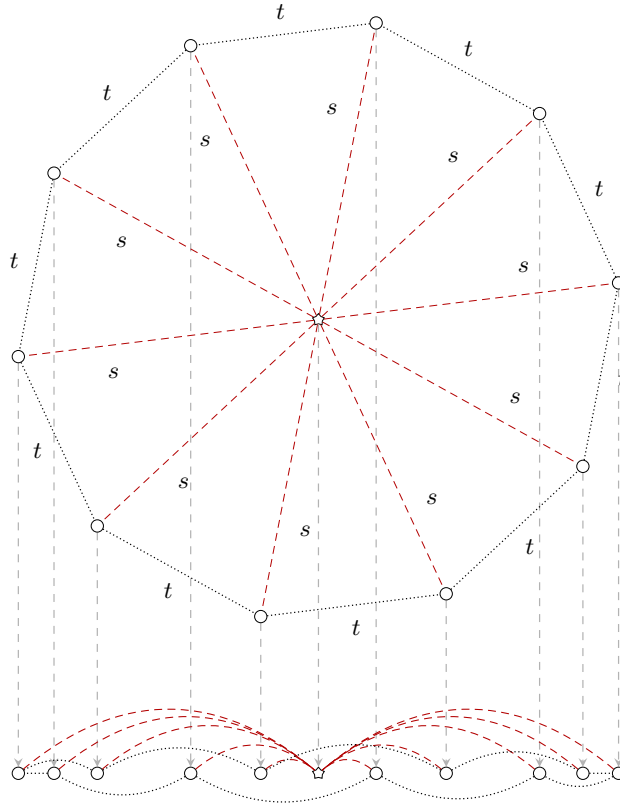


FIG. S1. Chosen projection of the wheel geometry (top) onto a chain (bottom). This reduces the long-range interaction from the first to the last site that is replaced by multiple next-nearest-neighbor interactions compared to a straight forward PBC implementation. The center site (star) of the wheel is placed in the middle of this chain – again in order to reduce the long-range interaction to a minimum.

All numerical results were obtained using the DMRG [45, 46] in its matrix-product state (MPS) representation [26] implemented in the SYMMPS toolkit [47]. More precisely, the calculations were performed with a bond dimension

up to 1200, which allowed the discarded weight to always stay below  $2 \cdot 10^{-8}$  and usually below  $10^{-10}$ . Since DMRG works best in one-dimensional (1D) systems, the wheel is projected onto a chain in a way that reduces the long-range interaction to a (rather large) minimum, see Fig. S1.

### Observables

The observable of interest, as shown in Fig. 4 in the main text, is the normalized condensate fraction of the distinguished  $k_0$ -mode extrapolated to the thermodynamic limit. Note that in our calculations we chose  $k_0 = 0$ . In order to obtain this quantity, we need to get the single-particle density matrix (SPDM) – in our case – of the ground state,

$$\rho_{j,j'} = \langle \hat{c}_j^\dagger \hat{c}_{j'} \rangle, \quad (\text{S40})$$

for multiple system sizes. The condensate fraction is then obtained by Fourier transforming the SPDM.

$$n_k = \frac{1}{L} \sum_{j,j'} e^{-2ik(j-j')/L} \rho_{j,j'}, \quad (\text{S41})$$

In order to be able to compare the condensate fractions for different system sizes, it is necessary to normalize them w.r.t the maximally possible value. This is given by [11]

$$n_{\max}(L) = (L - N + 1) \cdot N/L. \quad (\text{S42})$$

We chose four different sizes of the outer ring (32, 64, 128, 256) and extrapolated these normalized results via a  $1/L$  fit.

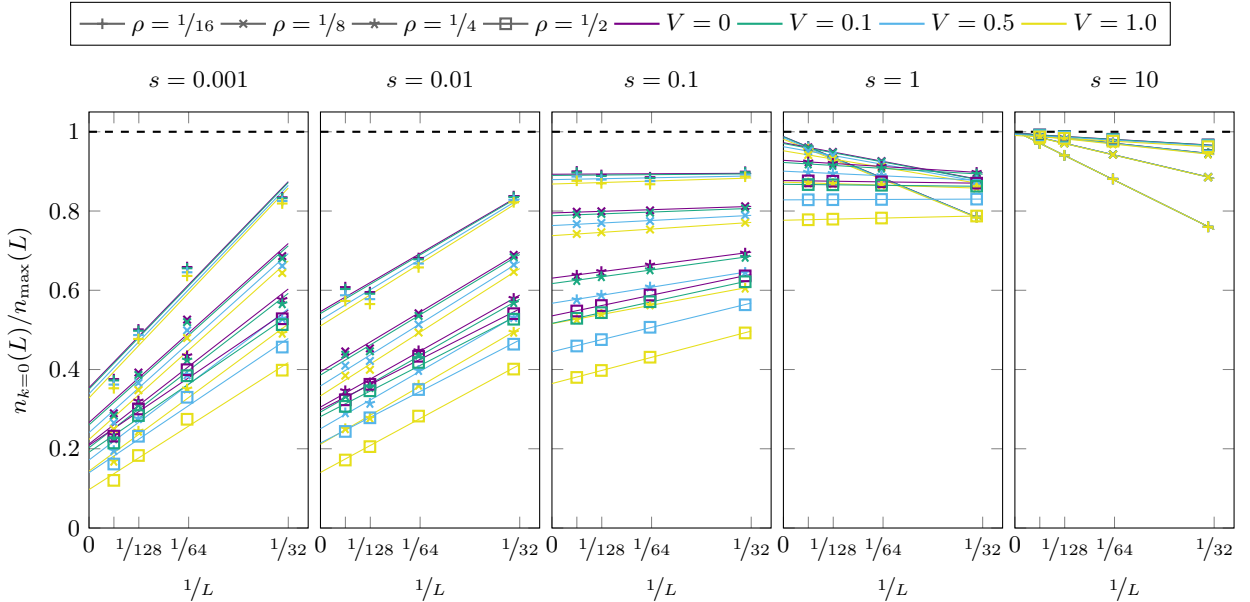


FIG. S2. Examples for the finite size scaling. For reasonably large densities, i.e., dense many-particle eigenstate clusters, we observe excellent  $1/L$  scaling to finite condensate fractions (normalized to the maximally possible condensate density  $n_{\max}(L)$ ). In the highly dilute limit, the many-particle spectrum is very sparse, causing an abrupt opening of the gap  $\Delta_2$ , which also effectively suppresses scatterings caused by the interactions.

In Fig. S2, a subset of the used data is shown, namely all data for  $s = 0.001, 0.01, 0.1, 1, 10$ . The chosen  $1/L$  fit is only valid if the density is large enough. This can be addressed to the fact that in the highly diluted regime the many-particle spectrum becomes very sparse and causes an abrupt opening of the gap  $\Delta_2$ . Also note that this sparseness can effectively suppresses the effect of interactions. Furthermore, the difference of the normalized condensate fraction w.r.t. the interaction strength becomes more pronounced the more particles can interact with each other. If the



ring-to-center hopping becomes too small ( $s < 10^{-2}$ ) additional effects come into play and interfere with the  $1/L$  fit. This can also be seen in Fig. S3, in which the fits for the highest density ( $\rho = 1/2$ ) and the highest interaction strength ( $V = 1$ ) are shown.

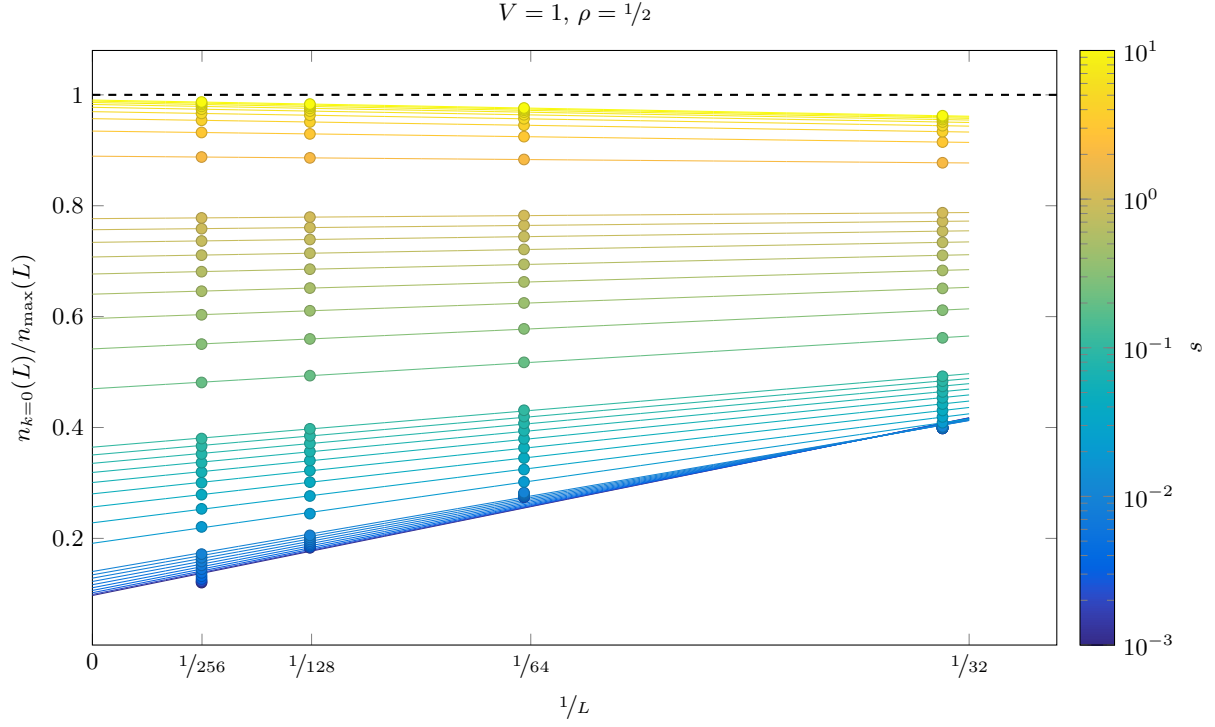


FIG. S3. Examples for the finite size scaling. For density  $\rho = 1/2$ , we observe excellent  $1/L$  scaling to finite condensate fractions (normalized to the maximally possible condensate density  $n_{\max}(L)$ ) for all ring-to-center hoppings larger than  $s > 10^{-2}$ .